International Journal of Materials and Chemistry 2015, 5(3): 54-63
DOI: 10.5923/j.ijmc.20150503.02

Modified Chitosan for Efficient Dye Adsorption in Low Acid Media

Nehal A. Salahuddin*, Mohamad M. Ayad, Magda E. Essa

Department of Chemistry, Faculty of Science, Tanta University, Tanta, Egypt

Abstract Polyoxypropylenediamine-modified chitosan (D_{2000}-Cs) was prepared by crosslinking of Cs by using epichlorohydrin (ECH) followed by chemical modification using D_{2000}. D_{2000}-Cs was characterized by X-ray diffraction (XRD), Fourier transform infrared (FT-IR), scanning electron microscopy (SEM), and thermal gravimetric analysis (TGA). The stability of D_{2000}-Cs in acid medium was also tested. The adsorption of an anionic dye, acid green 25 (AG) from acidic aqueous solution onto D_{2000}-Cs was investigated. The adsorption experiments were conducted by varying parameters namely: initial concentration of AG, pH and temperature. The kinetic models: pseudo-first order, pseudo-second order, and the intraparticle diffusion models were applied to the experimental data. The adsorption process was found to follow pseudo-second order kinetic model. The Langmuir, Temkin and Freundlich models were used to fit the adsorption isotherms. It was observed that the experimental data fits very well to the Langmuir model.

Keywords Polyoxypropylenediamine, Chitosan, Acid Green 25, Adsorption isotherm, Kinetics

1. Introduction

Colored organic effluent is produced in different industries such as textile, rubber, paper, plastic and cosmetics. The colored effluents of wastewater from these industries can be mixed in surface and ground water systems, and may transfer to drinking water and bring a chief threat to the human health due to their toxic or mutagenic and carcinogenic effects [1, 2]. Therefore, colored wastewater cannot be discharged without adequate treatment and dye removal. Physico-chemical processes such as coagulation and flocculation [3], membrane separation [4], oxidation [5], electro-coagulation [6], and adsorption on activated carbon and clays [7] were employed for the treatment of dye-containing wastewater. Among these methods, adsorption process is considered to be promising technology. Activated carbon is the most widely used commercial adsorbent due to its excellent adsorption capacity [8]. However, the high cost and the poor regeneration are the main drawbacks for the use of activated carbon as adsorbent [9]. Many studies were undertaken to find low cost sorbents such as cotton, fly ash, guava leaf powder, sugarcane bagasse pith, rice husk, and coconut coir [10-16].

Recently, most researchers concentrated towards natural polymeric materials, because they are renewable, biodegradable, non-toxic, and hence they are considered environment friendly materials [17]. Among the natural polymeric materials, chitosan (Cs) is the most attractive polymer due to its low cost and availability. Cs is a linear copolymer composed of (1–4)-linked D-glucosamine and N-acetyl-D-glucosamine and it is obtained by alkaline deacetylation of chitin (the second abundant polymer in nature after cellulose) [18]. Cs was widely used for the removal of heavy and transition metals [8, 19, 20] due to its high number of functional amines and hydroxyl groups, thus enabling the adsorption of anionic dyes through electrostatic attraction. However, Cs is soluble in dilute organic acids and is difficult to be separated from the solution using traditional separation methods such as filtration and sedimentation. To overcome such a problem, various physical and chemical modifications were developed to improve the chemical stability of Cs in acidic media. Recently, many researchers were interested in the chemical modification of Cs by cross-linking method using cross-linking agents such as glutaraldehyde [21, 22], epichlorohydrin (ECH) [23, 24] and ethyleneglycol diglycidyl ether [25, 26]. Although the crosslinking methods were found to enhance the resistance of Cs against acids, it reduced the adsorption capacity of Cs. To overcome this problem, the crosslinked Cs can be modified with Polyoxyalkylene diamines to increase the adsorption capacity.

The aim of the present work is directed to prepare a crosslinked Cs followed by modification with polyoxypropylenediamine (D_{2000}). Resultant D_{2000}-Cs has the advantage of improving the chemical stability of Cs in acidic media. D_{2000}-Cs was characterized using by X-ray diffraction (XRD), Fourier transform infrared (FT-IR),

* Corresponding author:
salahuddin.nehal@yahoo.com (Nehal A. Salahuddin)
Published online at http://journal.sapub.org/ijmc
Copyright © 2015 Scientific & Academic Publishing. All Rights Reserved

scanning electron microscopy (SEM) and thermal gravimetric analysis (TGA). Afterward, D_{2000}-Cs was tested for the adsorption of anionic dye, acid green 25 (AG) from acidic aqueous solutions. The effect of physicochemical parameters, that influence the adsorption process such as the initial concentration of AG, pH and temperature, were also investigated.

2. Experimental

2.1. Materials

Cs with a molecular weight of 100,000-300,000 and 90% degree of deacetylation (Acros, USA), ECH 99% (Acros, USA), Polyoxypropylene-diamine (D_{2000}) with molecular weight of 2000, primary amine content is 0.97 meq g^{-1} (Huntsman corporation TX, USA) were used without further purification. AG (Aldrich, UK), acetic acid and methanol (Adwic, EGYPT) and extra pure NaOH pellets (Lobachemie, INDIA) were used as received.

2.2. Preparation of D_{2000}-Modified Cs (D_{2000}-Cs)

The preparation of D_{2000}-modified Cs (D_{2000}-Cs) was carried out by the following steps:

2.2.1. Preparation of Cs Gel

The Cs gel was prepared using the previously reported method by Huang et al. [27]. Accordingly, a solution of Cs was prepared by dissolving 1 g of Cs in 33.3 ml of 2% acetic acid followed by drop wise addition of Cs solution to an alkaline precipitation bath (50 mL of 0.5 M NaOH aqueous solution). Afterward, the gelatinous precipitate of Cs was collected and washed for several times by distilled water then by ethanol to remove residual NaOH. Finally, the precipitate was stored in distilled water for further use.

2.2.2. Preparation of Crosslinked Cs

The Cs gel obtained from the previous step was suspended in 100 mL of a mixture of water–methanol (v/v, 1:1). Afterward, an excess amount of ECH (2 mL) was added drop wise to the suspension solution then the mixture was stirred at 60 °C for 24 h and cooled. Finally, the product was filtered and washed three times by water and ethanol to give crosslinked Cs (ECH-Cs) with nitrogen content 1.24 wt%.

2.2.3. Preparation of D_{2000}-Modified Cs (D_{2000}-Cs)

D_{2000}-Cs was prepared by suspending crosslinked Cs in 100 mL methanol/water mixture (1:1, v/v) followed by addition of 7.63 g D_{2000}. The reaction mixture was kept at 60°C with stirring for 24 h. Then, the product was filtered, washed three times by water and ethanol to remove the unreacted D_{2000} and dried at 60 ^{o}C. The product was finally grinded (Nitrogen content 4.31wt %).

2.3. Solubility Test

The solubility of D_{2000}-Cs was examined in acidic medium by adding 5 mg of the sample into 10 mL HCl (pH 2.3) for 24 h then the sample was reweighed.

2.4. Swelling Test

The D_{2000}-Cs sample was weighed in a sintered glass, W□ and then immersed in buffer solution (pH = 3, 5.4 and 7.8) at 25°C. After immersion, the sample was centrifuged and reweighed immediately, W_t. The process was repeated until W_t becomes constant. The swelling degree of the new material expressed as the amount of adsorbed buffer per 100 g of dry sample, the swellability percentage was calculated using the formula:

$$[(W_t - W_0) / W_0] \times 100 \quad (1)$$

2.5. Adsorption Batch Experiments

A stock solution of AG dye (186.8 mg L^{-1}) was prepared in freshly distilled water, and the solutions of desired concentrations (18, 23, 28, 31 and 36 mg L^{-1}) were obtained by successive dilution. Calibration curve was constructed by measuring the absorbance of the AG solutions at λ_{max} = 642 nm.

Adsorption experiments were carried out using 0.02 g of D_{2000}-Cs and ECH-Cs as adsorbents. For each experiment, 50 mL of AG dye solution (18 mg L^{-1}) along with the adsorbent were stirred magnetically (400 rpm) for 2, 5, 10, 15, 20, 25, 30, 35, 40, 50, 60 min at 25°C. The pH of the dye solution was adjusted to 3 for all the adsorption kinetic studies and equilibrium adsorption studies using 0.1 M HCl or 0.1 M NaOH. The samples of the dye solution, during the course of adsorption, were collected at regular intervals of time and centrifuged to remove the adsorbent.

The absorption spectra of dye solutions before and after adsorption were recorded in the range of 750 – 500 nm. The concentration of dye solutions were determined at a wavelength of λ_{max} = 642 nm. The quantity of adsorbed dye Q_e (mg g^{-1}) and the removal efficiency ($R\%$) were calculated from the following equations:

$$RE\% = [(C_0 - C_e) / C_0] \times 100 \quad (2)$$

$$Q_e = [(C_0 - C_e)\, V] / m \quad (3)$$

where, C_o is the initial dye concentration in liquid phase (mg L^{-1}), C_e is the liquid phase dye concentration at equilibrium (mg L^{-1}), V is the volume of dye solution (L), and m is the mass of adsorbent (g).

Kinetic analysis is required to obtain an insight of the rate of adsorption and the rate limiting step of the transport mechanism, which are primarily used in the modeling. In order to evaluate the kinetic mechanism that controls the adsorption process, the pseudo first order [28], pseudo second order [29, 30], and intraparticle diffusion [31] models were tested. The pseudo first order rate equation:

$$\log (Q_e - Q_t) = \log Q_e - (k_1 / 2.303)\, t \quad (4)$$

The pseudo second order reaction:

$$t / Q_t = (1/ k_2)\, Q_e^2 + t / Q_e \quad (5)$$

The intraparticle diffusion model [32]:

$$Q_t = k_i t^{1/2} + C \quad (6)$$

where, Q_t (mg g^{-1}) is the amount of dye adsorbed at time t (min), k_1 is the rate constant for pseudo first order, k_2 is the rate constant of the pseudo second order mode (g mg^{-1} min^{-1}), k_i is the intraparticle diffusion rate parameter (mg g^{-1} $min^{-1/2}$) and C is the intercept, which is proportional to the boundary layer thickness (mg g^{-1}). Good correlation with the kinetic data explains the dye adsorption mechanism in the solid phase.

The isothermal kinetics of the adsorption were described by isotherm models of which Langmuir [33], Freundlich [34], and temkin [35] are the most widely used equations.

The Langmuir adsorption isotherm in the linear form is expressed as:

$$C_e / Q_e = 1 / k_1 + a_1 C_e / k_1 \quad (7)$$

The Freundlich isotherm is expressed as:

$$\ln Q_e = \ln k_f + 1 / n \ln C_e \quad (8)$$

The Temkin isotherm is given by:

$$Q_e = B \ln k_T + B \ln C_e \quad (9)$$

where k_1 and a_1 are the Langmuir adsorption constants, k_f is the Freundlich adsorption constant, which roughly indicates the adsorption capacity of the adsorbent and n is the Freundlich constant, K_T is the equilibrium binding constant and B is a constant that is related to the heat of adsorption.

2.6. Instruments

The UV visible absorption spectra were measured using spectrometer, UVD-2960 (Labomed. INC). Fourier-transform infrared (**FT-IR**) spectra were recorded using Bruker, Tenson 27 FTIR spectrophotometer with frequency range of 4000 – 400 cm^{-1} using KBr disk technique. X-ray diffraction (XRD) analysis was measured by GNR, APD 2000 PRO step scan X-ray diffractometer, Cu Kα radiation (l.54 Å), (40 KV and 30 mA) at a step per second of 0.02°. Thermal gravimetric analysis (TGA) was carried out using Perkin Elmer, STA 6000. The morphology of crosslinked Cs and D_{2000}-Cs was studied by scanning electron microscope (SEM JEOL, JSM-5200LV) at an acceleration voltage of 25 KV. Quantitative elemental analysis for N in crosslinked Cs, D_{2000}-Cs was performed on Heraeus (microanalysis center, Cairo University, Giza, Egypt).

3. Results and Discussion

3.1. Synthesis and Characterization of D_{2000}-Cs

The aim of the present work is to produce a new material with high adsorption capacity and chemical stability in acid medium. To achieve this, Cs was dissolved in acetic acid to yield hydrogel in water. After that, Cs beads were crosslinked by using excess amount of ECH. Finally, the crosslinked Cs was modified by D_{2000}. Similar modification was reported using ethylenediamine [27]. The prepared D_{2000}-Cs showed satisfactory chemical stability in acid medium which was confirmed by its insolubility in strong acid media (pH = 2.3), however, Cs was completely soluble in weak acid medium.

The FT-IR spectrum of Cs (Figure. 1 (a)) shows a band at 3443 cm^{-1} due to the axial stretching vibration of OH superimposed to NH_2 stretching and inter- and intramolecular hydrogen bonding of Cs. The bands at 2921 and 2878 cm^{-1} are due to C–H asymmetric stretching vibration of CH_2 and C–H symmetric stretching vibration of CH_3 groups, respectively [36]. The band at 1646 cm^{-1} is assigned to C=O stretching of amide group ($NHCOCH_3$) due to partial deacetylation of chitin. The bands at 1603, 1460 and 1426 cm^{-1} are attributed to bending vibration of NH_2, CH_2, CH_3, respectively. The sharp peak at 1384 cm^{-1} is related to C–N stretch of amide group and CH_3 bending. The band at 1325 cm^{-1} refers to CH_2 scissoring and OH bending vibration [29]. The bands at 1259 and 1155cm^{-1} are due to C–N and the bridge C–O–C stretching vibrations, respectively, while the peaks at 1082 and 1028 cm^{-1} refer to C–O and CH_2OH stretching vibrations, respectively. The peak at 896 cm^{-1} is attributed to wagging of saccharine structure of Cs [37].

The FT-IR spectrum of the ECH-Cs, Figure. 1 (b) shows all the significant characteristic bands of Cs with some shifts in the position of bands. The same functional groups of the ECH were present in the Cs. Therefore, the same vibrations were observed, but with different intensities. The peak at 1646 cm^{-1} related to C=O stretch of amide group shifted to 1639 cm^{-1}. In addition, the band at 1603 cm^{-1} of NH_2 group disappeared which is a spectroscopic evidence for the covalent bonds formation between ECH and NH_2 groups of Cs. The peak at 1259 cm^{-1} related to C-N stretch became weak and shifted to 1255 cm^{-1} proving the introduction reaction of ECH on NH_2 position of Cs [37].

Significant changes were observed in the spectrum of D_{2000}-Cs presented in Figure. 1 (c). A band at 1603 cm^{-1} that is attributed to NH bending in primary amine groups (NH_2) was observed. The band at 2921 cm^{-1} related to asymmetric stretching vibration of C-H of CH_2 group shifted to 2973 cm^{-1} due to the insertion of D_{2000} into Cs. In addition, the bands at 1460 and 1384 cm^{-1} that are related to CH_2 bending and C–N stretching vibrations of amide group became more intense and shifted to 1456 and 1375 cm^{-1}, respectively. Furthermore, two new peaks appeared at 1301 and 1261 cm^{-1} due to the primary and secondary amino groups, which verify the grafting of D_{2000}.

The XRD pattern shown in Figure 2 (a) exhibits the characteristic crystalline peaks of Cs around 2θ of 10 and 20° [38-40]. After reaction with ECH, the peak at 2θ = 10° showed a pronounced disappearance and the peaks at 2θ = 10° and 20° became more broad due to the decrease in the crystallinity after crosslinking with ECH since amino groups were occupied [41]. In D_{2000}-Cs, a broad peak at 2θ = 20° was observed concomitant with the complete disappearance of the peak at 2θ = 10° due to the decrease in crystallinity, which indicates that Cs loses its structure registry due to the modification.

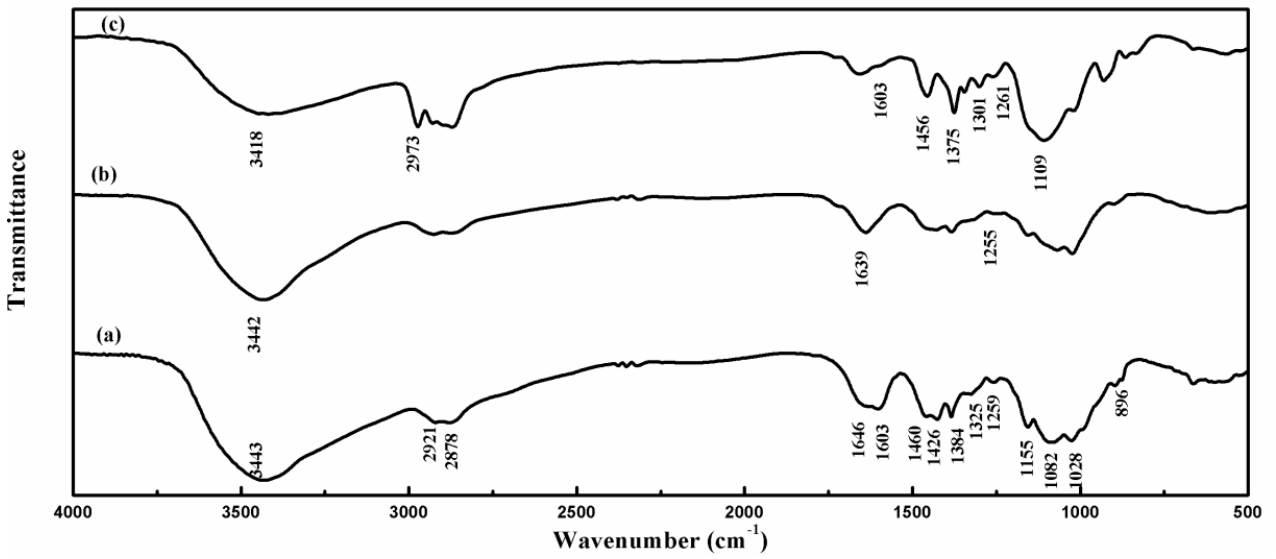

Figure 1. FTIR spectra of Cs (a), ECH-Cs (b) and D_{2000}-Cs (c)

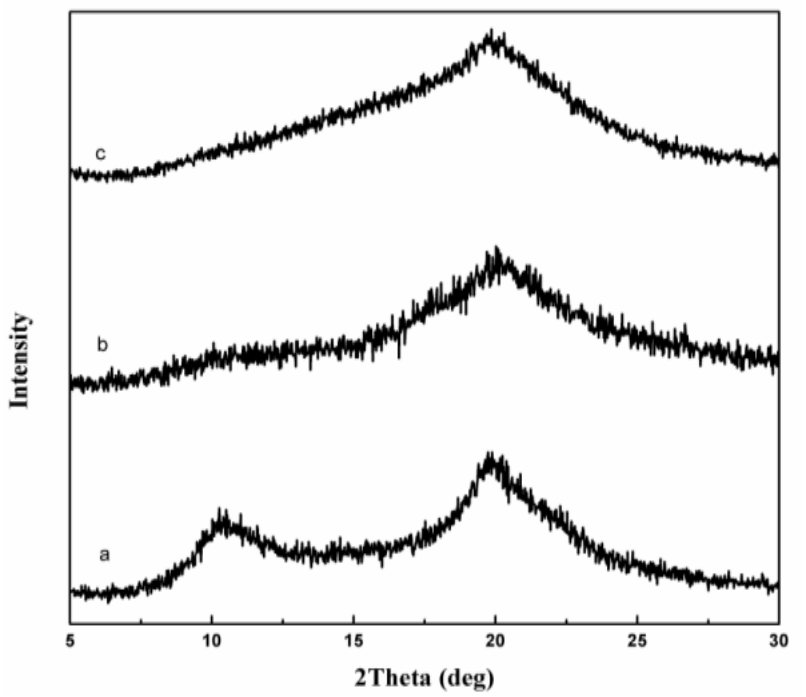

Figure 2. XRD spectra of Cs (a), ECH- Cs (b) and D_{2000}-Cs (c)

Figure. 3 shows the TGA curves of pure Cs, ECH-Cs and D_{2000}-Cs in the temperature range from 41 to 800°C. Weight losses of pure Cs occurred at three stages [42, 43]. The first stage started from 41 to 100°C with weight loss of 7.7 wt%. The second stage started from 250°C with loss of 42 wt% while, the third stage occurred from 350°C with weight loss of 47 wt%. The second and third stages correspond to the degradation of Cs chains and decomposition of pyranose rings with ring opening reaction respectively. Compared with the TGA curve of pure Cs, there are obvious alterations in crosslinked Cs and D_{2000}-Cs. The degradation temperature of crosslinked Cs shifted to lower temperature (200°C). This indicates that the reaction of Cs with ECH decreases the intermolecular and the intramolecular hydrogen bonding existed in Cs and hence decreases the thermal stability. However, in the D_{2000}-Cs, much weaker action between Cs and water molecules adsorbed in the sample was observed leading to a more stable material in the range from 41-210°C small weight loss. The high weight loss at 300-600°C could be attributed to the degradation of D_{2000}.

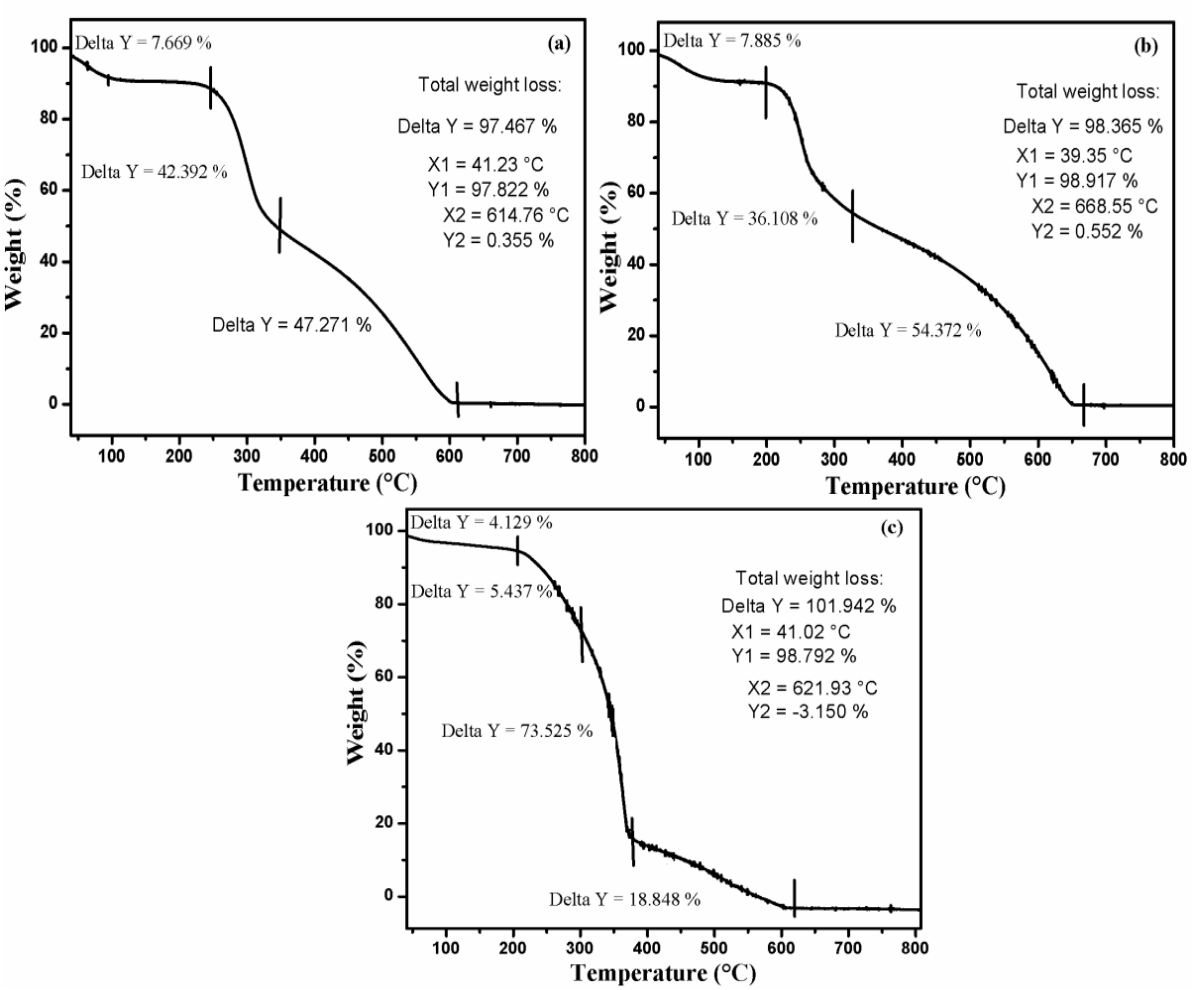

Figure 3. TGA of Cs (a), ECH- Cs (b) and D_{2000}-Cs (c)

The surface morphology of crosslinked Cs and D_{2000}-Cs were observed by SEM as shown in Figure. 4. The crosslinked Cs shows flaky structure however, D_{2000}-Cs shows accumulation of spherical domains with irregular surface morphology. This spherical morphology provides large surface area for adsorption.

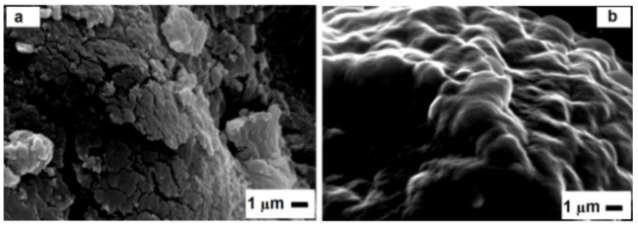

Figure 4. SEM of ECH- Cs (a) and D_{2000}-Cs (b)

The modification of ECH-Cs with D_{2000} lead to increase in the N content from 1.24 wt% to 4.31 wt% as indicated from the elemental analysis. The increase in N content caused an increase in the adsorption capacity of the adsorbent. In addition, it would be expected that the elasticity of D_{2000} favors the adsorption capacity of modified Cs. The D_{2000}-Cs was found to be insoluble in acid medium in comparison to the native Cs. The swelling of D_{2000}-Cs was evaluated to be 248%, 137% and 124% at pH 3, 5.4 and 7.8, respectively. These values confirm its stability in buffer solution (no weight loss).

3.2. Adsorption of AG onto D_{2000}-Cs

The D_{2000}-Cs can be utilized as an ideal material for acidic wastewater treatment that includes anionic dyes. To investigate the effect of crosslinking and modification by D_{2000} on the adsorption of dyes, experiments were conducted for adsorption at pH = 3 from 50 mL of 18 mg L^{-1}AG with 20 mg of ECH-Cs and D_{2000}-Cs.

Table 1. Adsorption capacity (Q_e), adsorptivity (R%) of D_{2000}-Cs and ECH-Cs

Adsorbent	Q_e (mg g^{-1})	R%
D_{2000}-Cs	44.5	99.4
ECH-Cs	6.5	14.4

Figure. 5 shows the adsorption capacity against time using D_{2000}-Cs and ECH-Cs. It is clear that D_{2000}-Cs exhibited much higher adsorption capacity as compared to that of crosslinked Cs. The amount of dye adsorbed per unit mass (Q_e) of D_{2000}-Cs and crosslinked Cs were, 44.5 and 6.5 mg g^{-1} with adsorbtivity ($R\%$) equals 99.4 and 14.4%, respectively showed in table 1. This may be attributed to the

high surface area of D_{2000}-Cs and the large number of binding sites (NH_2 groups), which lead to high interaction between AG and the D_{2000}-Cs. In addition, the loading of D_{2000} improves the adsorptivity. Amine groups can significantly uptake the AG in acid medium through electrostatic interaction between NH_3^+ and O^- in AG.

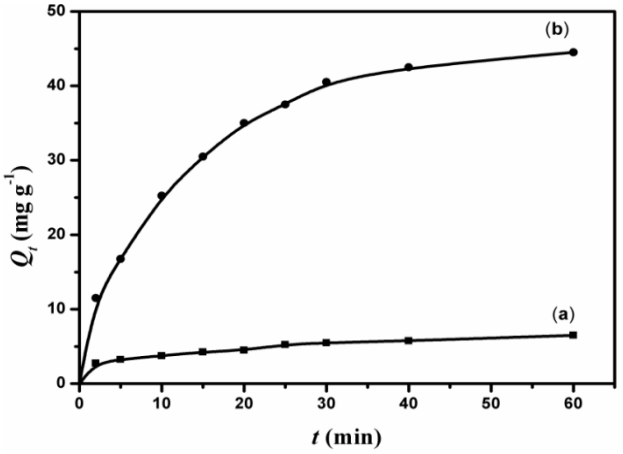

Figure 5. Adsorption capacity of ECH- Cs (a) and D_{2000}-Cs (b)

3.3. Adsorption Kinetics

The kinetic analysis, in order to evaluate the kinetic mechanism that controls the adsorption process, were tested by applying the pseudo first order [28], pseudo second order [29, 30] and intraparticle diffusion [31]. Figure. 6 (a-c) shows the corresponding linear plots. The parameters, k_1, Q_e, K_2 and the correlation coefficient (R^2) were determined and presented in Table 2. The results of the regression analysis showed that the adsorption of AG dye onto D_{2000}-Cs was best described by pseudo-second order with the highest correlation coefficients.

Table 2. Kinetic parameters for the adsorption of AG onto D_{2000}-Cs

Model	Parameters	$R^{2\,a}$
Pseudo first order	Q_e = 50.12 mg g^{-1} k_1 = 0.09 min^{-1}	0.96
Pseudo second order	Q_e = 52.63 mg g^{-1} k_2 = 0.002 g mg^{-1} min^{-1}	0.996
Intra particle diffusion	k_i = 5.5 mg g^{-1} min^{-1} C = 6.5 mg g^{-1}	0.95

[a] Correlation coefficient

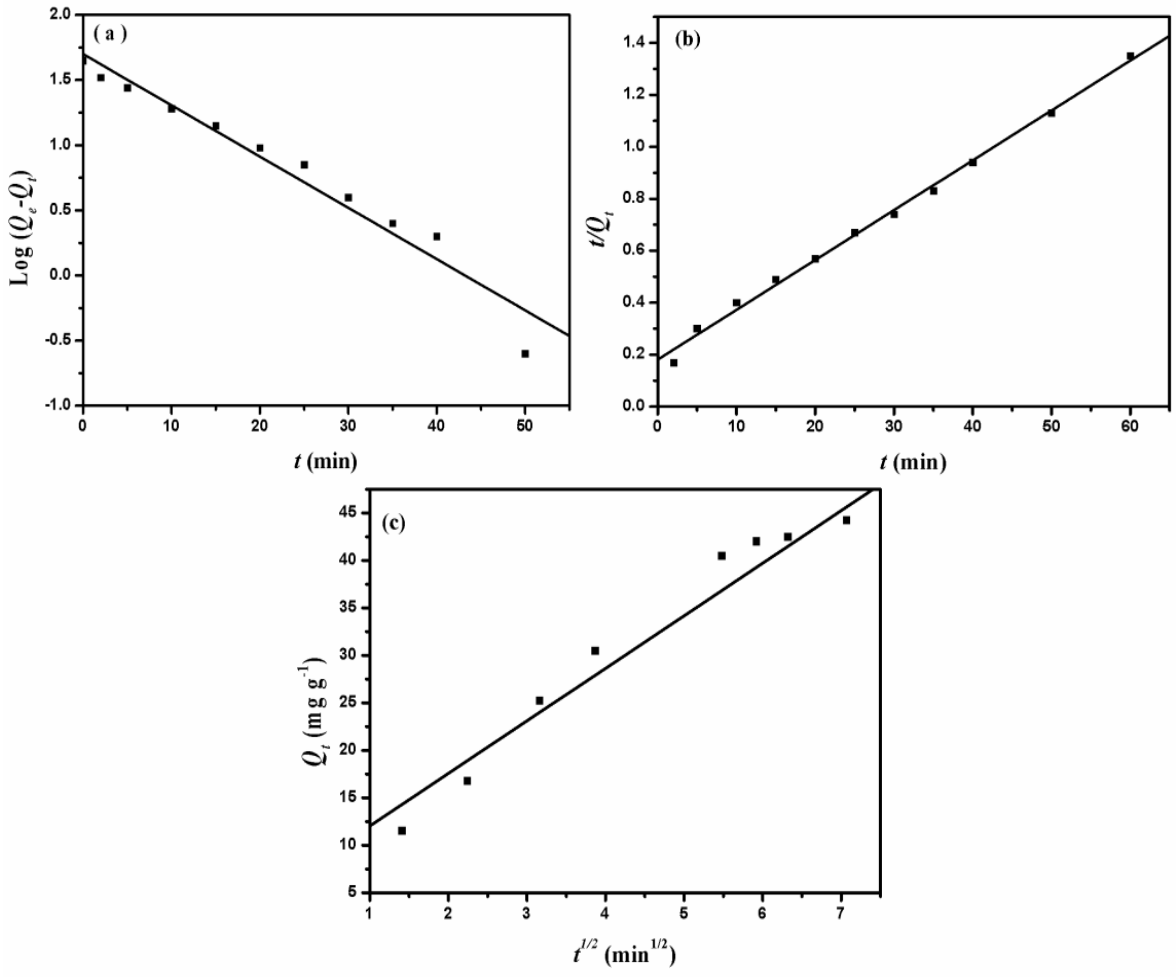

Figure 6. The pseudo first order (a), pseudo-second-order (b) and Intraparticle diffusion kinetic plots for adsorption of AG onto D_{2000}-Cs

3.4. Adsorption Isotherms

Table 3. Isotherm parameters of adsorption of AG on D_{2000}-Cs

Model	Parameters	$R^{2\ a}$
Langmuir	Q_o = 62.5 mg g^{-1} K_l = 3333.3 L g^{-1} a_l = 53.3 L mg^{-1} R_l = 0.00078	0.98
Freundlich	K_f = 56.3 L g^{-1} n = 11.11	0.83
Temkin	K_T = 3.36 L mg^{-1} B = 5.1	0.80

[a] Correlation coefficient

The adsorption isotherms of the adsorption of AG into D_{2000}-Cs were studied. The most common sorption models used to fit the experimental data are Langmuir [33], Freundlich [34], and Temkin [35], are showed in Figure. 7 and the correlation coefficient (R^2) was calculated and reported in Table 3. For the three studied systems, R^2 of Langmuir isotherm is more near to unity and is better than R^2 of Freundlich and Temkin isotherms. Hence, the Langmuir model is the most widely used for the sorption of AG onto D_{2000}-Cs.

Figure. 7 (d) shows the variation of separation factor (R_l) with initial AG concentrations (C_o). The results exhibited that R_l values were in the range of 0–1, indicating that the adsorption AG onto D_{2000}-Cs is favorable.

3.5. The Effect of pH

The pH of the dye solution plays an important role in the whole adsorption process, particularly affecting the adsorption capacity. Figure. 8 shows that the amount of dye adsorbed onto D_{2000}-Cs increased with decreasing pH of solution. At lower pH, more protons will be available for the protonation of NH_2 groups in D_{2000} or Cs leads to increasing the electrostatic attraction force between D_{2000}-Cs and dye molecules. At high pH, the protonation of the amino groups decreases and leads to decrease adsorption [44]. The values of Q_e for the adsorption of AG dye solution onto D_{2000}-Cs at pH = 3, 4.5, 7 and 9 were 40.5, 32, 28 and 16 mg g^{-1}, respectively.

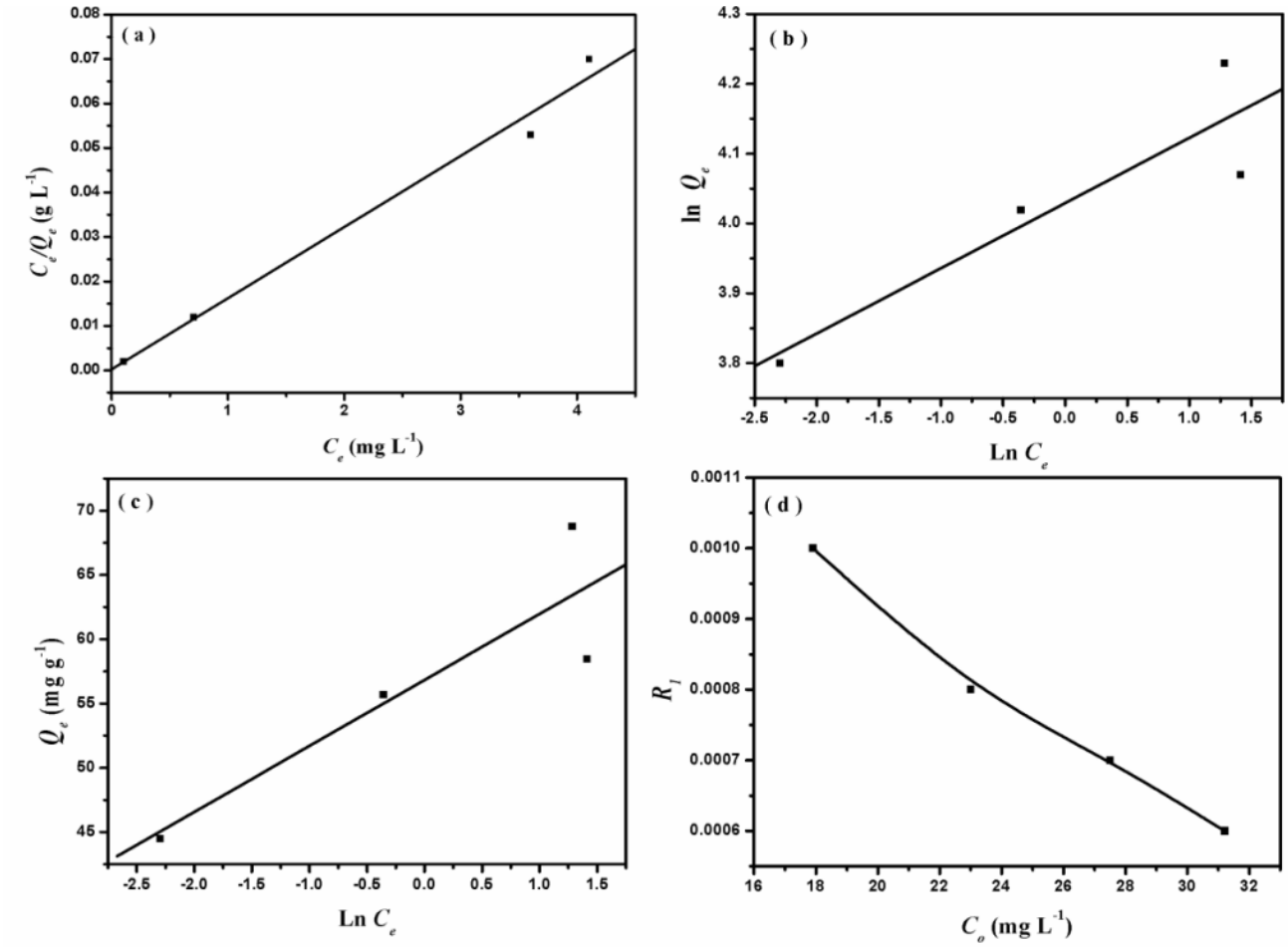

Figure 7. Langmuir isotherm model (a), Freundlich isotherm model (b), Tempkin isotherm model (c) and separation factor versus initial AG concentration (d)

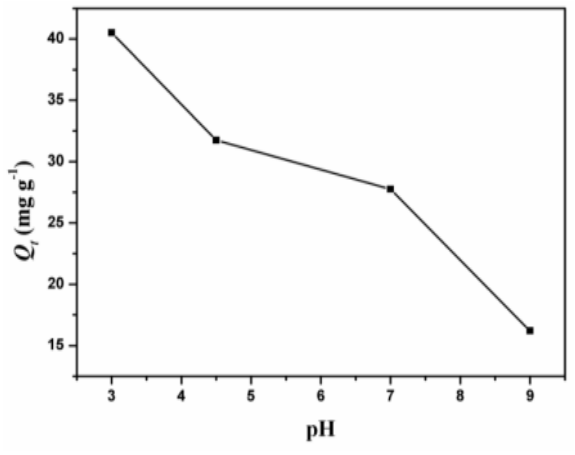

Figure 8. Adsorption of AG onto D_{2000}-Cs at different pH

3.6. The Effect of Initial Dye Concentration

Figure. 9 shows the effect of initial dye concentration (C_o) on the adsorption kinetics of the D_{2000}-Cs. The initial pH of dye solution was adjusted to 3. The values of Q_e for the adsorption of AG dye solution (50 ml) with concentrations 18, 23, 31 and 36 mg L^{-1} using D_{2000}-Cs (0.02 mg) are 44.5, 55.4, 69 and 84 mg g^{-1}, respectively. Figure. 9 shows that the adsorption capacity increases with increasing C_o.

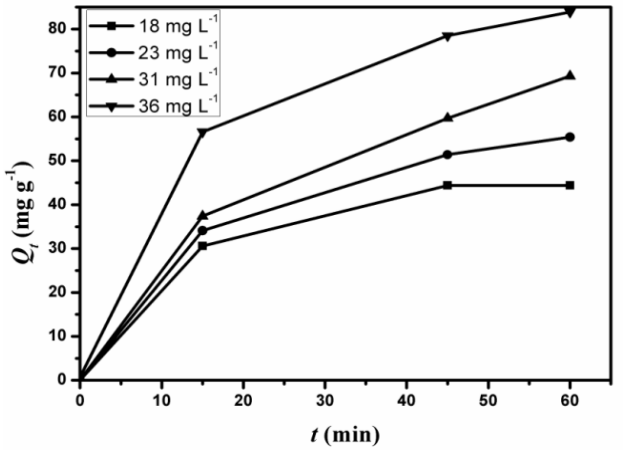

Figure 9. Effect of initial concentration on the adsorption of AG by D_{2000}-Cs

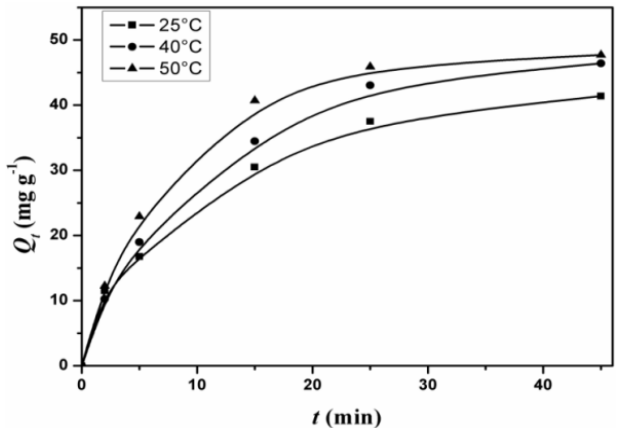

Figure 10. Effect of temperature on the adsorption of AG onto the D_{2000}-Cs

3.7. The Effect of Temperature

The effect of temperature on the adsorption capacity of AG onto D_{2000}-Cs was studied at pH = 3 and the results are shown in Figure. 10. The adsorption capacity increased with increasing temperature from 25 to 50°C, which indicates the endothermic nature of the adsorption process.

4. Conclusions

Cs was modified by using polyoxypropylenediamine (D_{2000}) to obtain (D_{2000}-Cs). The product was tested for the adsorption of anionic dye, acid green 25 (AG), from acidic aqueous solutions and shows good stability. The adsorption ability of D_{2000}-Cs for removal of anionic dyes in acid medium is efficient and overcomes the drawbacks of using Cs as adsorbent due to its solubility in acid medium.

The initial concentration of AG, pH and temperature significantly affect the adsorption process and the adsorption capacity of D_{2000}-Cs. The Langmuir model agrees very well with the equilibrium isotherm and the pseudo-second order describe the equilibrium kinetics.

REFERENCES

[1] Chiou, M. S., Ho, P., Ho, Y., and Li, H. Y., 2004, Adsorption of anionic dyes in acid solutions using chemically cross-linked chitosan beads, Dyes Pigm, 60, 69–84.

[2] Wan-Ngah, W. S, Teong, L. C., and Hanafiah, M. A. K. M., 2011, Adsorption of dyes and heavy metal ions by chitosan composites: A review, Carbohydr. Polym., 83, 1446–1456.

[3] Sadri-Moghaddam, S., Alavi-Moghaddam, M. R., and Arami, M., 2010, Coagulation/flocculation process for dye removal using sludge from water treatment plant: optimization through response surface methodology, J. Hazard. Mater., 175, 651–657.

[4] Jirankova, H., Mrazek, J., Dolecek, P., and Cakl, J., 2010, Organic dye removal by combined adsorption–membrane separation process, Desalin. Water Treat., 20, 96-101.

[5] Sundararaman, T. R., Ramamurthi, V., and Partha, N., 2009, Decolorization and COD removal of reactive yellow 16 by fenton oxidation and comparison of dye removal with photo fenton and sono fenton Process, Mod. App. Sci., 3, 15–22.

[6] Eyvaz, M., Kirlaroglu, M., Aktas, T. S., and Yuksel, E., 2009, The effects of alternating current electrocoagulation on dye removal from aqueous solutions, Chem. Eng. J., 153, 16–22.

[7] Li, W. H., Yue, Q. Y., Gao, B. Y., Ma, Z. H., Li, Y. J., and Zhao, H. X., 2011, Preparation and utilization of sludge based activated carbon for the adsorption of dyes from aqueous solutions, Chem. Eng. J., 171, 320–327.

[8] Crini, G., 2006, Non-conventional low-cost adsorbents for dye removal: a review, Bioresour. Technol., 97, 1061–1085.

[9] Sakkayawonga, N., Thiravetyana, P., and Nakbanpoteb, W., 2005, Adsorption mechanism of synthetic reactive dye

wastewater by chitosan, J. Colloid. Interface Sci., 286, 36–42.

[10] Chairata, M., Rattanaphanib, S., Bremnerc, J. B., and Rattanaphanib, V., 2008, Adsorption kinetic study of lac dyeing on cotton, Dyes Pigm, 76, 435–439.

[11] Lin, J. X., Zhan, S. L., Fang, M. H., Qian, X. Q., and Yang, H., 2008, Adsorption of basic dye from aqueous solution onto fly ash, J. Environ. Manage., 87, 193–200.

[12] Ponnusami, V., Vikram, S., and Srivastava, S. N., 2008, Guava (Psidiumguajava) leaf powder: novel adsorbent for removal of methylene blue from aqueous solutions, J. Hazard. Mater., 152, 276–286.

[13] Amin, N. K., 2008, Removal of reactive dye from aqueous solutions by adsorption onto activated carbons prepared from sugarcane bagasse pith, Desalin. Water Treat., 223, 152–161.

[14] Han, R., Ding, D., Xu, Y., Zou, W., Wang, Y., Li, Y., Zou, L., 2008, Use of rice husk for the adsorption of congo red from aqueous solution in column mode, Bioresour. Technol., 99, 2938–2946.

[15] Sureshkumar, M. V., and Namasivayam, C., 2008, Adsorption behavior of direct red 12B and Rhodamine B from water onto surfactant-modified coconut coir pith, Colloids Surf. A., 317, 277–283.

[16] Cheung, W. H., Szeto, Y. S., and McKay, G., 2007, Intraparticle diffusion processes during acid dye adsorption onto chitosan, Bioresour. Technol., 98, 2897–2904.

[17] Chang, M. Y., and Juang, R. S., 2004, Adsorption of tannic acid, humic acid, and dyes from water using the composite of chitosan and activated clay, J. Colloid. Interface Sci., 278, 18–25.

[18] Synowiecki, J., and Al-Khateeb, N. A., 2003, Production, properties, and some new applications of chitin and its derivatives, Cri.t Rev. Food Sci. Nutr., 43, 145–171.

[19] Vieira, R. S., and Beppu, M. M., 2006, Interaction of natural and crosslinked chitosan membranes with Hg (II) ions, Colloids Surf. A., 279, 196–207.

[20] Salam, M. A., Makki, M. I., and Abdelaal, M. Y. A., 2011, Preparation and characterization of multi-walled carbon nanotubes/chitosan nanocomposite and its application for the removal of heavy metals from aqueous solution, J. Alloys. Compd., 509, 2582–2587.

[21] Poon, L., Wilson, L. D., and Headley, J. V., 2014, Chitosan-glutaraldehyde copolymers and their sorption properties, Carbohyd. Polym., 109, 92–101.

[22] Cestari, A. R., Vieira, E. F. S., Tavares, A. M. G., and Bruns, R. E., 2008, The removal of the indigocarmine dye from aqueous solutions using cross-linked chitosan–Evaluation of adsorption thermodynamics using a full factorial design, J. Hazard. Mater., 153, 566–574.

[23] Li, C. G., Wang, F., Peng, W. G., He, Y. H., 2013, Preparation of Chitosan and Epichlorohydrin Cross-Linked Adsorbents and Adsorption Property of Dyes, Apll. Mech. Mater, 423-426, 584-587.

[24] Yeng, C. M., Husseinsyah, S., and Ting, S. S., 2015, A comparative study of different crosslinking agent-modified chitosan/corn cob biocomposite films, Polym. Bull., 72, 791-808.

[25] Li, N., and Bai, R., 2005, Copper adsorption on chitosan–cellulose hydrogel beads: behaviors and mechanisms, Sep. Purif. Technol., 42, 237–247.

[26] Wanngah, W. S., Ghani, S. A., and Kamari, A., 2005, Adsorption behaviour of Fe(II) and Fe(III) ions in aqueous solution on chitosan and cross-linked chitosan beads, Bioresour. Technol., 96, 443–450.

[27] Huang, X. Y., Bin, J. P., Bu, H. T., Jiang, G. B., and Zeng, M. H., 2011, Removal of anionic dye eosin Y from aqueous solution using ethylenediamine modified chitosan, Carbohydr. Polym., 84, 1350–1356.

[28] Wu, F. C., Tseng, R. L., and Juang, R. S., 2001, Kinetic modeling of liquid-phase adsorption of reactive dyes and metal ions on chitosan, Water Res., 35, 613–618.

[29] Chiou, M. S., and Li, H. Y., 2002, Equilibrium and kinetic modeling of adsorption of reactive dye on cross-linked chitosan beads, J. Hazard. Mater., 93, 233–248.

[30] Ho, Y. S., and McKay, G., 1999, Pseudo-second order model for sorption processes, Process Biochem., 34, 451–465.

[31] Uzun, İ., 2006, Kinetics of the adsorption of reactive dyes by chitosan, Dyes Pigm, 70, 76–83.

[32] Weber, W. J., and Morris, J. C., 1963, Kinetics of Adsorption on Carbon from Solution, J. Sanit. Eng. Div., Am. Soc. Civ. Eng., 89, 31–59.

[33] Langmuir, I., 1918, The adsorption of gases on plane surfaces of glass, mica and platinum, J. Am. Chem. Soc., 40, 1361–1403.

[34] Poots, V. J. P., McKay, G., and Healy, J. J., 1978, Removal of basic dye from effluent using wood as an adsorbent, J. Water Pollut. Control Fed., 50, 926–935.

[35] Tempkin, M. J., and Pyzhev, V., 1940, Recent modifications to Langmuir isotherms, Acta Phys. Chim., 12, 217–222.

[36] Silva, S. M. L., Braga, C. R. C., Fook, M. V. L., Raposo, C. M. O., Carvalho, L. H., and Canedo, E. L., 2012, In:Tech Theophile, T. (ed) 2nd, 51, 978–953.

[37] Heydarzadeh, H. D., Najafpour, G. D., Nazari-Moghaddam, A. A., 2009, Catalyst-free conversion of alkali cellulose to fine carboxymethyl cellulose at mild conditions, World App. Sci. J., 4, 564–569.

[38] Zhou, T. F. J. J., Zhou, J. X., Gao, L. H., Xing, Y. Y., and Li, X. H., 2011, Synthesis and characterization of chitosan-based schiff base compounds with aromatic substituent groups, Iran. Polym. J., 2, 123–136.

[39] Samuels, X. R. J., 1981, Solid state characterization of the structure of Cs films, J. Polym. Sci., Polym. Phys. Ed., 19, 1081–1105.

[40] Ogawa, K., Yui, T., and Miya, M., 1992, Dependance and the preparation procedure of polymorphism and crystallinity of Cs membranes, Biosci. Biotechnol. Biochem., 56, 858–862.

[41] Tang, X., Zhang, X., Guo, C., and Zhou, A., 2007, Adsorption of Pb^{2+} on Chitosan Cross-Linked with triethylene-tetramine, Chem. Eng. Technol., 30, 955–961.

[42] Gao, X., Zhou, Y., Ma, G., Shi, S., Yang, D., Lu, F., and Nie, J., 2010, A water-soluble photocrosslinkable chitosan

derivative prepared by Michael addition reaction as a precursor for injectable hydrogel, Carbohydr. Polym., 79, 507–512.

[43] Zhang, C., Ping, Q., Zhang, H., and Shen, J., 2003, Synthesis and characterization of water-soluble O-succinyl-chitosan, Eur. Polym. J., 39, 1629–1634.

[44] Chiou, M. S., and Li, H. Y., 2003, Adsorption behavior of reactive dye in aqueous solution on chemical cross-linked chitosan beads, Chemosphere, 50, 1095-1105.